Journal of
Marine Science and Engineering

Article

Laboratory Experiments on the Influence of the Wave Spectrum Enhancement Factor on a Rubble Mound Breakwater

Hosny Bakali [1,*], Ismail Aouiche [1], Najat Serhir [1], Youssef Zahir [2], El hassan Ziane [3], Abderrazak Harti [3], Zakariae Zerhouni [3] and Edward Anthony [4]

[1] Er-SHEMSS, Laboratory of Civil Engineering, Hydraulics, Environment and Climat, Hassania School of Public Works, Casablanca 20000, Morocco
[2] Civil Engineering Company SOMAGEC, Corner Mohamed El Mesfioui & Corbi, Casablanca 20580, Morocco
[3] Public Laboratory for Studies and Tests, Casablanca 20000, Morocco
[4] CNRS, IRD, INRA, Coll France, CEREGE, Aix Marseille University, 13545 Aix-en-Provence, France
* Correspondence: albakalihosny@gmail.com

Abstract: This paper experimentally explored the influence of the wave spectrum shape variation on breakwater design. The energy spectrum function generally considered for the design of coastal structures is the JONSWAP spectrum. The laboratory results were therefore used to assess the impact of changing the spectrum shape parameter (*PEF*). We analysed armour stability and wave overtopping in a wave flume with a geometric similarity ratio of 1:30. The experimental results showed that the *PEF* has maximum influence on overtopping and wave pressures on the crown wall. For a *PEF* value of 3.3, overtopping was much higher (30% to 100% higher) than with a *PEF* of 1. Pressure on the crown wall was 20% higher with a *PEF* of 3.3 in comparison with that for a *PEF* equal to 1. The stability of the breakwater's block armour is less sensitive to the *PEF* variation.

Keywords: energy spectrum; JONSWAP spectrum; peak enhancement factor; wave flume; overtopping; breakwater design

Citation: Bakali, H.; Aouiche, I.; Serhir, N.; Zahir, Y.; Ziane, E.h.; Harti, A.; Zerhouni, Z.; Anthony, E. Laboratory Experiments on the Influence of the Wave Spectrum Enhancement Factor on a Rubble Mound Breakwater. *J. Mar. Sci. Eng.* **2022**, *10*, 2035. https://doi.org/10.3390/jmse10122035

Academic Editors: Giovanni Ludeno and Matteo Postacchini

Received: 14 November 2022
Accepted: 9 December 2022
Published: 19 December 2022

1. Introduction

Breakwaters are frequently used to protect beaches and coastal infrastructure, notably ports and marinas. Breakwaters play a crucial role in reducing wave energy that could cause potential damage to installations located inside ports, especially during storms when setup can lead to overtopping [1,2]. There are several types of breakwaters, but rubble mound breakwaters are the most widely used because of their ability to dissipate swell energy [3] as well as their relatively low cost and easy maintenance [4,5]. However, notwithstanding these advantages, armour layer failures can occur due to the stochastic nature of wave loading [6], thus leading to the initiation of damage [7]. Physical modelling is therefore an important and reliable approach in finally reaching an approvable breakwater design. Physical tests are generally conducted in order to identify different failure modes such as movements of the armour layer blocks, failure of the crown wall, and the propensity for overtopping flow [8,9]. Proper modelling of irregular waves during physical tests is a crucial step towards obtaining accurate results; hence, an initial study of local wave parameters must be conducted to define wave parameters based on in situ wave measurements and numerical ocean meteorology models [10].

Irregular waves are generally described by the significant wave height (*Hs*), i.e., the average wave height of the highest one-third of the waves. The Rayleigh distribution of wave heights is universally employed for their description [11]. However, overtopping, wave loading, and structural response depend not only on wave heights but also on wave periods [8]. Determining the distributions of wave heights and periods is crucial to ensure a safe and operational structure.

To reproduce the distribution of wave heights and periods, the wave train is modelled using a theoretical spectrum that depicts the distribution of wave energy as a function of frequencies. The wave spectrum can be expressed in terms of significant wave height (H_s), peak frequency (f_p) or peak period (T_p) ($f_p = 1/T_p$), and of form parameters such as the Peak Enhancement Factor (*PEF*) [12]. Several spectral functions are used to represent the wave signal: Jonswap, Pierson-Moskowitz [13], ISSC, ITTC, JONSWAP, SCOTT, and Liu [14]. Among these, the Jonswap spectrum is one of the most widely used for different sea conditions. The JONSWAP spectrum was established following a series of tests in the North Sea carried out by Hasselmann et al. [15]. This spectral density function of wave energy is currently the most adopted for the design of coastal structures because the shape parameters of this function can be set to match the shape of the wave spectrum with the local wave energy distribution. In the case of the Moroccan Atlantic coast, no study has been conducted thus far to define the local wave spectrum model of offshore waves. Mean spectral shape parameters are commonly considered for the design of different types of breakwaters; nevertheless, the choice of an inappropriate shape parameter may lead to underestimation or overestimation of breakwater stability during physical tests.

Recent studies have examined the influence of the wave spectrum variation on the design of coastal protection structures. Sensitivity studies reveal the influence of wave direction, height and *PEF* on harbour agitation and on wave setup inside port basins [16,17]. Zhang et al. [18] conducted physical modelling tests on a vertical breakwater and highlighted a significant impact of wave spectrum forms. In comparison to a wide wave spectrum, a narrow spectrum generates higher pressures on a caisson surface. Palemón-Arcos et al. [19] conducted wave flume tests to study the impact of narrow and wide spectra on vertical caisson stability, and revealed larger displacements of the caisson for a narrow energy spectrum. Van der Meer et al. [20] experimentally showed that wave overtopping due to a single peak spectrum (in particular the JONSWAP spectrum) depended mainly on the peak period T_p, or period with highest spectral energy density. For another function form of spectrum energy such as a double peak spectrum, Schtittrumpf et al. [21] and Van der Meer [22] showed the pertinence of the spectral wave period $T_{m-1,0}$. In fact, $T_{m-1,0}$ gives more weight to the longer periods in the spectrum than an average period.

The objectives of this study are to investigate the influence of the *PEF* variation on the stability of a rubble mound breakwater, as well as its influence on overtopping flow. Physical model tests on a rubble mound breakwater were conducted in a wave flume. Physical tests are carried out as part of the studies on the construction of the Dakhla Atlantic New Port (DANP project) in southern Morocco.

2. Materials and Methods

2.1. Model Set-up

All of the tests were conducted in the wave flume of the Moroccan Public Laboratory of Studies and Tests (CEH-LPEE) in Casablanca. We carried out the tests in a 1.05 m-wide and 44 m long wave flume; the maximum modelled water depth allowed by flume facilities is 1.4 m (cf. Figure 1). The side concrete walls of the flume are equipped with glazed panels to facilitate observations of wave propagation and photography. A series of three resistance type wave gauges were placed along the channel according to the recommendations of Mansard and Funk [23]. The wave flume, a schematic view of which is depicted in Figure 2, is equipped with a generator of random waves, and the wave board has an absorption system at the end of the canal. This means that the motion of the wave board compensates the waves reflected by the structure and prevents them from re-reflecting at the wave board and propagating towards the model. The reference level is the zero tide level (Zh) from which all other tide levels are measured. The wave generator is located at a water depth corresponding to -25 m/Zh, and the foot of the experimental breakwater, the object of the study, at a depth corresponding to -17 m/Zh. The bottom of the wave flume is made of concrete. The modelled water depth corresponding to -25 m/Zh varies from

0.974 m, corresponding to the tide level + 4.21 m/Zh, to 0.954 m, corresponding to the tide level + 3.61 m/Zh.

(**a**) (**b**)

Figure 1. Photo of the wave flume with the model breakwater in the foreground (**a**) and components of the breakwater (**b**) front slope (1), crown wall (2), and back slope (3).

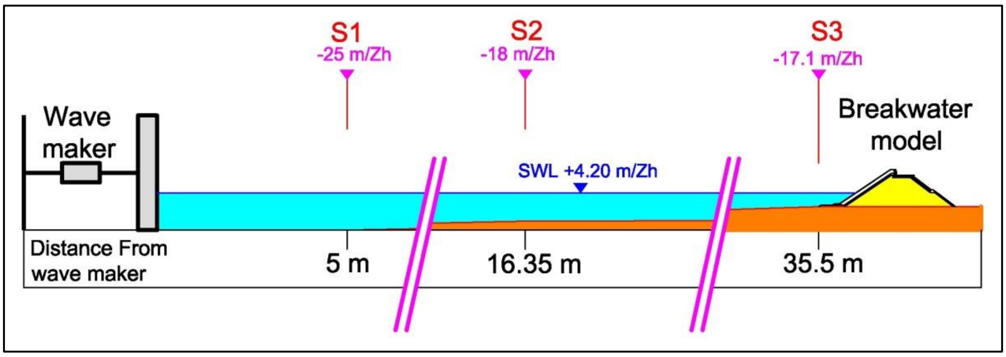

Figure 2. Schematic view of the wave flume physical model.

The breakwater armour blocks are made of Cubipods®with a unit volume of 3 m^3 placed on the wave-exposed side, and a reduced volume of 1.5 m^3 in the upper part of the rear slope. Cubipod®is a novel precast block that can be placed in a single or double layer; and it has an economical advantage in comparison with commonly used blocks such as tetrapods and Antifer blocks. Cubipods®have a proven ability of resistance to a large range of wave conditions in the Mediterranean Sea and the Atlantic Ocean [24]. The breakwater core is made of rubble components ranging in weight from 1 to 1000 kg; a stone layer separates the core from the armour blocks. Figure 3 presents a cross section of the studied breakwater.

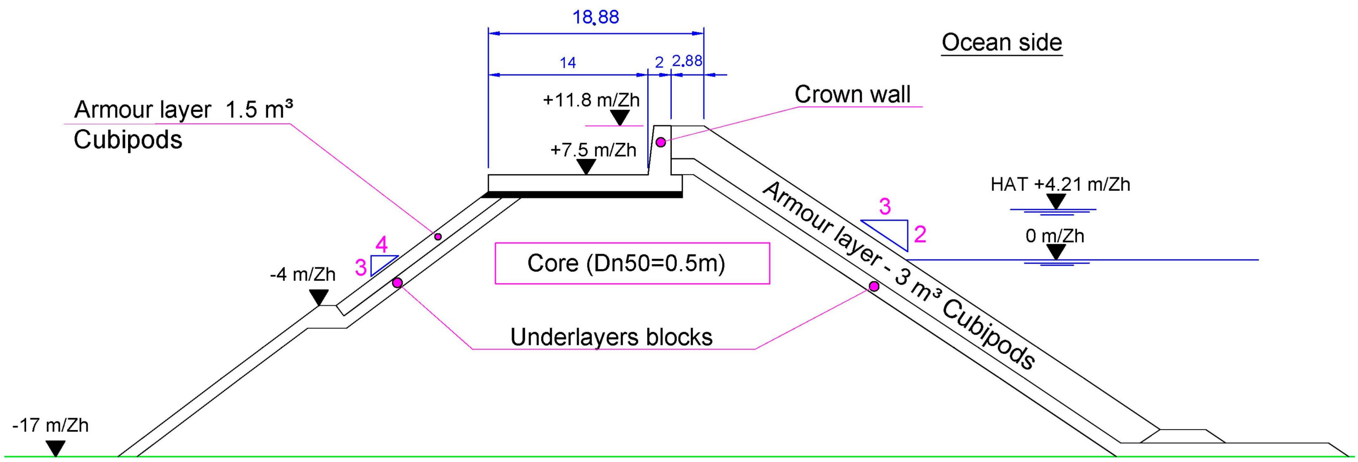

Figure 3. Section of the experimental rubble mound breakwater.

Experimental reproductions of breakwater geometry and wave conditions are conducted with respect to a Froude similarity law according to Kirkegaard et al. [25], with a similarity factor of $N = 30$. The resulting scaling factors are presented in Table 1.

Table 1. Scaling factors resulting from a Froude similarity law.

Notation	Unit	Scaling Factor
Length, width, wave height	m	N
Surface	m^2	N^2
Volume	m^3	N^3
Time	s	$N^{1/2}$
Velocity	m/s	$N^{1/2}$
Mass	kg	N^3
Density	kg/m^3	1

Considering the scaling factors presented in Table 1, the natural and modelled material properties are shown in Table 2.

Table 2. Material properties of the model breakwater relative to a full-scale breakwater.

Test Reference	Density (kg/m^3)	Full-Scale Median Weight (kg)	Modelled Median Weight (kg)
Front armour layer	2.4	7200	0.267
Rear armour layer	2.4	3600	0.133
Underlayer in front side	2.6	600	0.022
Underlayer in rear side	2.6	350	0.013
Core	2.6	500	0.018

Short tests were carried out to calibrate the wave spectrum at the location of S1 gauge (Cf. Figure 2). In order to avoid wave scattering due to breakwater wave reflection, these tests were conducted in the absence of the structure.

2.2. Wave Spectrum

The energy spectrum density according to the JONSWAP model [15] is written in the form:

$$S(f) = \frac{\alpha g^2}{(2\pi)^4 f^5}\, e^{\left(-\frac{5}{4}\left(\frac{f_p}{f}\right)^4\right)} \gamma^r \tag{1}$$

where

- $r = e^{[-\frac{(f-f_p)^2}{2\sigma^2 f_p^2}]}$
- α: Phillips constant
- f_p is the frequency which corresponds to the peak value of the spectral density function
- σ = (σ_a if $f \leq f_p$; σ_b if $f \geq f_p$)

Goda [11] proposed an approximate formula that takes into account the wave characteristics ($H_{1/3}$ and $T_{1/3}$)

$$S(f) = \beta_J \times H_{1/3}^2 \times T_P^{-4} \times f^{-5} \times e^{(-1.25 \times (T_p \times f)^{-4})} \times \gamma^r \tag{2}$$

where

- $\beta_J = \frac{0.0624 \times (1.094 - 0.01915 \times \ln \gamma)}{0.23 + 0.0336\gamma - 0.185(1.9+\gamma)^{-1}}$
- $r = e^{[-\frac{(f-f_p)^2}{2\sigma^2 f_p^2}]}$
- γ varies from 1 to 7
- $H_{1/3}$: Significant wave height
- $T_{1/3}$: Significant wave period
- T_p: Peak period.

The values of the wave form parameters (σ and γ) vary with the transformation of the spectrum form during wave propagation. High values of γ are recorded near the wave generation zone as a result of the concentration of wave energy around the peak frequency (f_p) [15]. During wave propagation, nonlinear interactions between waves involves energy transfer from peak frequencies to low wavelengths and very long wavelengths [26,27].

Considering the variation of the *PEF* values from 7 for a very narrow spectrum to 1 for a wide spectrum in the nearshore zone, a mean value of γ = 3.3 is commonly adopted for wave modelling [15,28]. In this study, we carried out physical model tests for the JONSWAP spectrum with the commonly used γ of 3.3, and also tested the influence of a γ of 1, which may correspond to the most realistic value for the coastal area in southern Morocco [28].

2.3. Wave Conditions

The required security level for rubble mound breakwaters implies a design for the 100-year return period wave height [5], while larger return periods allow for higher security with lower failure probability during the structure's lifetime. In the particular case of the DANP project, the project sponsors decided on a minimum of a 100-year return period wave height design; in addition, verifications for a 200-year return period wave height were also recommended in order to avoid potential major damages.

All tests were conducted for irregular waves. Simulations corresponded to wave heights for the aforementioned 100 and 200-year return period events, and different periods (T_p), as well as the retained *PEF* (γ = 1 and γ = 3.3). The duration of the tests covered a period sufficiently long to represent a real sea state. The natural wave conditions retained are summarized in Table 3.

Table 3. 100- and 200-year return period of natural wave conditions.

Test Reference	Return Period	T_p (s)	*PEF*	H_s
DAK21135	200 years	14	1	6 m
DAK21136	200 years	14	3.3	6 m
DAK21137	100 years	16	3.3	5.5 m
DAK21139	100 years	16	1	5.5 m
DAK21138	100 years	18	3.3	5.5 m

Table 3. *Cont.*

Test Reference	Return Period	T_p (s)	*PEF*	H_s
DAK21146	100 years	18	1	5.5 m
DAK21154	200 years	16	3.3	6 m
DAK21155	200 years	16	1	6 m
DAK21156	200 years	18	3.3	6 m
DAK21157	200 years	18	1	6 m

2.4. Measurements of Damage, Pressure on the Crown Wall and Overtopping

Armour damage on mound breakwaters is determined by visual observations of block displacements [29]. According to Losada et al. [30] and Vidal et al. [31], four levels of damage are generally observed:

- Beginning of damage: Corresponds to the displacements of the armour blocks over a distance greater than or equal to D_{50} (mean diameter of armour blocks);
- Irribaren damage: Holes created in the armour surface cause the exposure of the sub-layer;
- Beginning of destruction: Corresponds to the beginning of damage to the sub-layer;
- Destruction: the sub-layer is exposed to the effect of incident waves.

To improve damage visualization, we took a series of photographs enabling measurement of potential damage inception and growth (before, during and after tests). The movement of the CUBIPODS® was recorded using a high-precision digital video camera. After each test, the moved and flipped units were counted before reconstituting the layer for the next test. In order to measure the instantaneous variation of wave pressure on the crown wall, the latter was equipped with a sensor placed at mid-height (Cf. Figure 4).

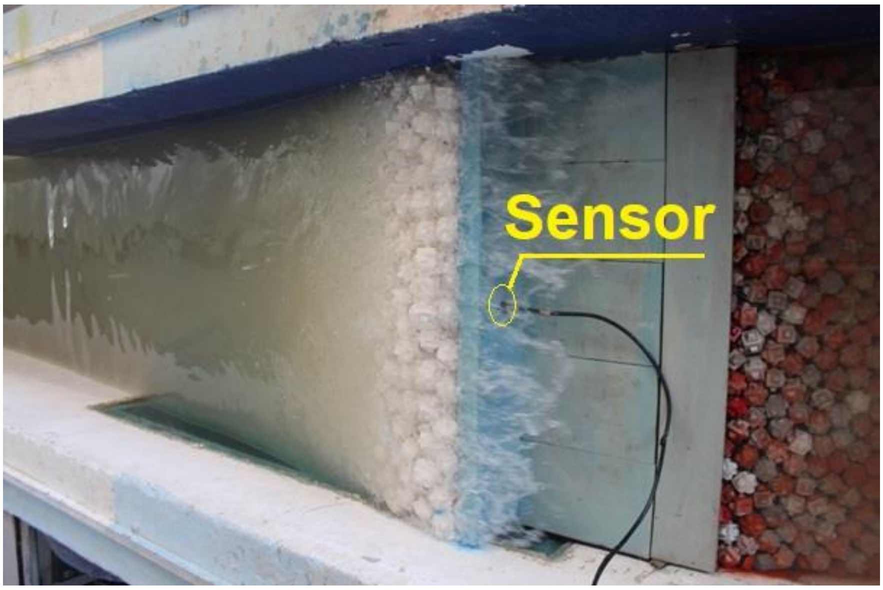

Figure 4. Location of the pressure sensor to measure the instantaneous variation of wave pressure impact on the crown wall.

The overtopping discharge was measured with a receptacle placed next to the crown wall. Measurements consisted in determining the total volume of discharge caused by N incident waves corresponding to the duration of a storm [29].

The mean overtopping is determined by the formula (3):

$$Q = \frac{V}{B \times T} \tag{3}$$

where

- V: Total of the overtopping volume measured at the end of the test
- B: Width of the receptacle
- T: Test duration.

3. Results

3.1. Overtopping

Table 4 summarizes the mean overtopping discharge (Q) values measured in the course of the various return-period set of tests.

Table 4. Results of the average overtopping flow.

Test	Return Period	T_p [s]	γ	H_s	Q (L/s/m)
DAK21137	100 years	16	3.3	5.5	26
DAK21139	100 years	16	1	5.5	19
DAK21138	100 years	18	3.3	5.5	46
DAK21146	100 years	18	1	5.5	24
DAK21154	200 years	16	3.3	6	62
DAK21155	200 years	16	1	6	41
DAK21156	200 years	18	3.3	6	88
DAK21157	200 years	18	1	6	43

Figure 5 depicts a graphical comparison between mean overtopping for significant wave heights of Hs = 5.5 m and Hs = 6 m, for the two peak periods of 16 and 18 seconds, and for the PEF values of γ = 1 and γ = 3.3.

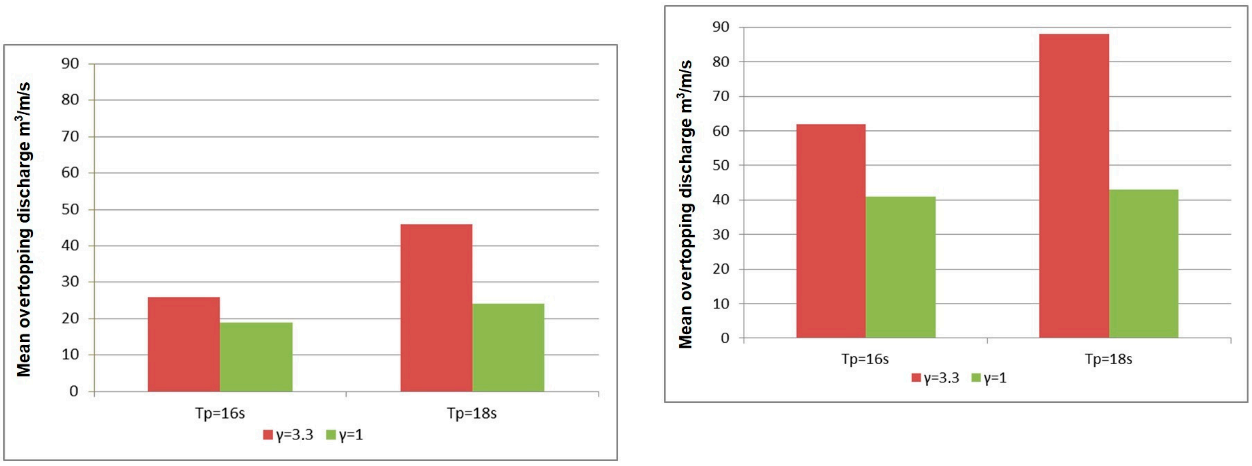

(**a**) (**b**)

Figure 5. Results of the mean overtopping flow for Hs = 5.5 m (**a**) and Hs = 6 m (**b**).

The results highlight the following points:

- The measured average overtopping rate (q) for a spectrum with γ = 3.3 is 35% to 100% greater than with the spectrum with γ = 1.
- For a wave spectrum generated with γ = 1, the measured average overtopping has almost the same value for the two peak periods T_p = 16 s and T_p = 18 s.

3.2. Water Pressure on the Crown Wall

The graph in Figure 6 shows a comparison of the maximum pressures on the crown wall measured for the three peak periods of 14 s, 16 s, and 18 s. All tests were carried out with a significant wave height *Hs* = 6 m. The analysis of the influence of the *PEF* variation can be supplemented by the study of other peak periods.

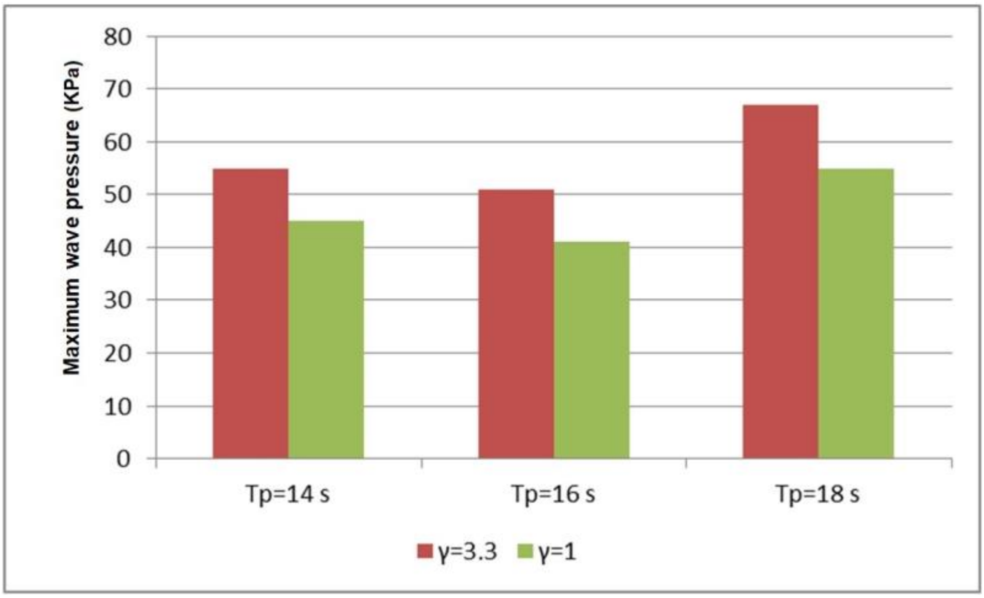

Figure 6. Maximum pressures of waves with *Hs* = 6 m for different values of peak periods.

The results highlight the following points:

- For a given value of the peak period (T_p), the measured maximum pressure for a spectrum with γ = 3.3 is 20% higher than the spectrum with γ = 1.
- For a given value of the *PEF*, the maximum peak period generated the higher value of maximum wave pressure.

3.3. Armour Block Stability

Wave attack for the two *PEF* parameters 1 and 3.3 was examined in the stability tests. The block displacements and damages were observed visually and are identified in the photographs which are summarized in Table 5.

Table 5. Block armour stability.

Water Level [m/Zh]	H_s (In −25 m/Zh)	T_p (In −25 m/Zh)	Observations for γ = 3.3	Observations for γ =1
+4.21	4 m	12 s	No damage	No damage
+3.61	4.4 m	14 s	No damage	No damage
+4.21	5 m	12 s	No damage	No damage
+4.21	5 m	18 s	No damage	No damage
+3.61	5 m	18 s	No damage	No damage
+4.21	5.5 m	14 s	Oscillation of 2 blocks	Oscillation of 1 block
+4.21	5.5 m	18 s	Oscillation of 2 blocks	Oscillation of 2 blocks
+ 3.61	5.5 m	18 s	Oscillation of 2 blocks	Oscillation of 2 blocks
+ 4.21	6 m	18 s	Extraction of 3 blocks	Oscillation of 3 blocks
+ 3.61	6 m	18 s	Extraction of 3 blocks	Oscillation of 4 blocks
+ 4.21	6.6 m	18 s	Extraction of 3 blocks	Oscillation of 4 blocks

Based on the damage results obtained from the physical model tests, we note that:

- For the first tests established for waves with *Hs* varying from 4 to 5 m, the variation of the *PEF* parameter has no consequence on armour stability. This is mainly due to the fact that the structural response is below the threshold of the damage beginning level;

- For the rest of the tests where we approached the destabilization limits (*Hs* varying from 5 to 6 m), we noted that the influence of the *PEF* becomes more meaningful for higher peak periods.

However, these observations require further tests using different types of armour and different wave conditions to determine the degree of the influence of the *PEF* parameter on armour layer stability.

4. Discussion

The measurements carried out in the experiments were obtained for a single breakwater section; therefore, care should be taken in generalizing the results. These results are, however, valid for similar structural and natural conditions. These results highlight a significant influence of the *PEF* variation on the maximum pressures measured for the three peak periods. Pressure on the crown wall was 20% higher for a wave spectrum with a *PEF* of 3.3 in comparison with the case of a spectrum with a *PEF* of 1. The variation of the measured maximum pressure is not mainly due to the variation of the maximum wave height for different wave spectra. In fact, the variation in the distribution of wave heights is slightly sensitive to the variation of the *PEF* factor. Rayleigh [32] proposed a general model for the distribution of wave heights as described by Equation (4); this wave height distribution is valid for all spectrum forms (or all PEF values):

$$f(H) = \frac{\pi}{2} \times \frac{H}{H_{mean}^2} \times e^{\left(\frac{-\pi}{4} \times \frac{H^2}{H_{mean}^2}\right)} \quad (4)$$

Goda [33] studied the impact of the variation of the *PEF* of the JONSWAP spectrum on the distribution of wave heights. Based on the results of Goda [33], Table 6 shows the ratio between mean wave height (H_{mean}), significant wave height (H_S or $H_{1/3}$), and the mean of the 10% highest waves ($H_{1/10}$).

Table 6. Relation between H_{mean}, H_s, and $H_{1/10}$ for different wave heights distributions.

	γ =1	**γ =3.3**	**Rayleigh Distribution**
$H_{1/10}/H_s$	1.248	1.253	1.271
H_{mean}/H_s	0.639	0.636	0.626

The difference between the $H_{1/10}$ heights for the two studied JONSWAP spectra with γ = 3.3 and γ = 1 is approximately 1%. This difference cannot be the source of the measured pressure differences. The variation of maximum wave pressure on the crown wall is therefore due to other factors associated with the spectral energy distribution.

For all performed tests, the armour layer remains in the beginning level of damage. It is necessary, therefore, to conduct other tests with higher wave height values. These tests may enable the comparison of stability results in situations with higher damage levels. However, the results obtained in our experiments show that in the case where the spectral energy is concentrated in long ocean swell waves with high peak periods (*Tp* = 18 s), such as may be encountered on the Atlantic coast of Morocco, the variation of the peak enhancement factor could influence the stability of concrete armour layers.

5. Conclusions

The accurate design of coastal structures requires knowledge of local spectral shape parameters determined from in situ wave measurements [12]. Where wave data are lacking, the assumption generally made is the consideration of standard shape parameter values [15,34]. This hypothesis is inappropriate for a rigorous design of coastal structures; indeed, previous studies depicted the influence of the *PEF* on vertical breakwaters [18,19].

This research highlights the influence of the spectral shape parameter (*PEF*) on rubble mound breakwater design. Physical tests are conducted for a breakwater located in intermediate water depth ($0.05 \leq d/L \approx 0.08 \leq 0.5$; where d and L are the local depth and wave length respectively [35]), with significant overtopping flow (20 L/m/s < Q < 80 L/m/s). Swell conditions considered are described with significant wave height from 5 to 6 m, and peak periods from 14 to 18 s. Consequently, the results obtained are valid for the natural range of conditions of this project.

Keeping in mind the precautions evoked above regarding generalization of the results obtained, we draw the following conclusions from the analysis of the experimental results:

- The *PEF* variation has a significant effect on the pressure exerted on vertical structures and on mean overtopping flow;
- The stability of the armour layers is not sensitive to the variation of the *PEF* for intermediate wave periods (12 to 14 s). This observation is consistent with the results of armour stability tests conducted by Van der Meer and Pilarczyk [36] for narrow and wide wave spectra. However, for longer waves, higher values of the *PEF* lead to more severe damage levels. The influence of the *PEF* on armour layer response is therefore highlighted for long period ocean waves.

Depending on the wave conditions, different spectra can be adopted to describe the irregular wave. The JONSWAP spectrum is commonly used for the description of irregular waves. Our study reveals that the shape parameters of the JONSWAP spectrum have a significant influence on rubble mound breakwater design. Therefore, the local shape characterization of the wave spectrum is necessary to ensure the stability and reliability of the structural design.

Author Contributions: Conceptualization, H.B., I.A. and N.S.; methodology, E.h.Z. and A.H.; validation, N.S. and E.A.; Performing tests, Z.Z.; resources, Y.Z.; writing—original draft preparation, H.B.; writing—review and editing, H.B., I.A., E.A. and N.S.; supervision and project administration, N.S. All authors have read and agreed to the published version of the manuscript.

Funding: This research received no external funding.

Institutional Review Board Statement: Not applicable.

Informed Consent Statement: Not applicable.

Data Availability Statement: Not applicable.

Acknowledgments: We thank the public laboratory for studies and tests and the directorate of ports and the maritime public domain for their valuable participation. We thank the two reviewers for their constructive suggestions.

Conflicts of Interest: The authors declare that they have no conflict of interest.

References

1. Mares-Nasarre, P.; Molines, J.; Gómez-Martín, M.E.; Medina, J.R. Individual wave overtopping volumes on mound breakwaters in breaking wave conditions and gentle sea bottoms. *Coast. Eng.* **2020**, *159*, 103703. [CrossRef]
2. van Gent, M.R.; Wolters, G.; Capel, A. Wave overtopping discharges at rubble mound breakwaters including effects of a crest wall and a berm. *Coast. Eng.* **2022**, *176*. [CrossRef]
3. Takahashi, S. *Design of Vertical Breakwaters*; Version 2.1; Port and Airport Research Institute: Kanagawa, Japan, 2002; (revised July 2002).
4. Burcharth, H.F.; Andersen, T.L.; Lara, J.L. Upgrade of coastal defence structures against increased loadings caused by climate change: A first methodological approach. *Coast. Eng.* **2014**, *87*, 112–121. [CrossRef]
5. CIRIA; CETMEF. *L'utilisation des Enrochements Pour les Ouvrages Hydrauliques-Version Française*, 2nd ed.; CETMEF: Compiègne, France, 2009.
6. Nielsen, S.R.K.; Burcharth, H.F. Stochastic design of rubble mound breakwaters. In *System Modelling and Optimization*; Springer: Berlin/Heidelberg, Germany, 1984; pp. 534–544. [CrossRef]
7. Campos, Á.; Molina-Sanchez, R.; Castillo, C.; Molina-Sanchez, R. Damage in rubble mound breakwaters. Part I: Historical review of damage models. *J. Mar. Sci. Eng.* **2020**, *8*, 317. [CrossRef]
8. Van der Meer, J.W.; Allsop, N.W.H.; Bruce, T.; De Rouck, J.; Kortenhaus, A.; Pullen, T.; Zanuttigh, B. *Manual on Wave Overtopping of Sea Defences and Related Structures*; Van der Meer Consulting: Delft, the Netherlands, 2018. Available online: http://www.overtopping-manual.com/ (accessed on 4 May 2021).

9. Pepi, Y.; Romano, A.; Franco, L. Wave overtopping at rubble mound breakwaters: A new method to estimate roughness factor for rock armours under non-breaking waves. *Coast. Eng.* **2022**, *178*. [CrossRef]
10. DHI. *Spectral Waves FM Module-User Manual*, 10th ed.; Danish Hydrological Danish Institute: Hørsholm, Denmark, 2012. Available online: www.mikepoweredbydhi.com/products/mike-21/waves (accessed on 30 June 2021).
11. Goda, Y. *Random Seas and Design of Maritime Structures*, 2nd ed.; World Scientific Pub Co Pte Ltd.: Singapore, 2000; Volume 15. [CrossRef]
12. Ewans, K.; McConochie, J. Optimal methods for estimating the Jonswap spectrum peak enhancement factor from measured and hindcast data. In Proceedings of the Offshore and Arctic Engineering-OMAE2019, Glasgow, UK, 9–14 June 2019. [CrossRef]
13. Pierson, W.J., Jr.; Moskowitz, L. A proposed spectral form for fully developed wind seas based on the similarity theory of S. A. Kitaigorodskii. *J. Geophys. Res. Space Phys.* **1964**, *69*, 5181–5190. [CrossRef]
14. Chakrabarti, S.K. *Hydrodynamics of Offshore Structures*, 5th ed.; Computational Mechanics Publications: Boston, MA, USA, 2001.
15. Hasselmann, K.; Barnett, T.P.; Bouws, E.; Carlson, H.; Cartwright, D.E.; Enke, K.; Ewing, J.A.; Gienapp, A.; Hasselmann, D.E.; Kruseman, P.; et al. *Measurements of Wind-Wave Growth and Swell Decay during the Joint Sea Wave Project (JONSWAP)*; Deutsches Hydrographisches Institute: Hamburg, Germany. Available online: https://hdl.handle.net/21.11116/0000-0007-DD3C-E. (accessed on 21 August 2021).
16. Gao, J.; Ma, X.; Zang, J.; Dong, G.; Ma, X.; Zhu, Y.; Zhou, L. Numerical investigation of harbor oscillations induced by focused transient wave groups. *Coast. Eng.* **2020**, *158*, 103670. [CrossRef]
17. Gao, J.; Ma, X.; Dong, G.; Chen, H.; Liu, Q.; Zang, J. Investigation on the effects of Bragg reflection on harbor oscillations. *Coast. Eng.* **2021**, *170*, 103977. [CrossRef]
18. Zhang, Q.; Zhai, H.; Wang, P.; Wang, S.; Duan, L.; Chen, L.; Liu, Y.; Jeng, D.-S. Experimental study on irregular wave-induced pore-water pressures in a porous seabed around a mono-pile. *Appl. Ocean Res.* **2020**, *95*, 102041. [CrossRef]
19. Palemón-Arcos, L.; Torres-Freyermuth, A.; Pedrozo-Acuña, A.; Salles, P. On the role of uncertainty for the study of wave–structure interaction. *Coast. Eng.* **2015**, *106*, 32–41. [CrossRef]
20. Van Der Meer, J.W.; Tönjes, P.; De Waal, J.P. A Code for Dike Height Design and Examination. In Proceedings of the Coastlines, Structures and Breakwaters Conference, London, UK, 19–20 March 1998; pp. 5–19. [CrossRef]
21. Schüttrumpf, H.; Möller, J.; Oumeraci, H.; Grüne, J.; Weissmann, R. Effects of Natural Sea States on Wave Overtopping of Seadikes. In Proceedings of the Fourth International Symposium on Ocean Wave Measurement and Analysis, San Francisco, CA, USA, 2–6 September 2001. [CrossRef]
22. TAW. *Technisch Repport Golfoploop En Golfoverslag Bij Dijken/Wave Run-Up and Wave*; Technical Advisory Committee on Flood Defence: Delft, The Netherland, 2002.
23. Mansard, E.P.; Funke, E.R. The measurement of incident and reflected spectra using a least squares method. In Proceedings of the 17th Coastal Engineering Conference, Sydney, Australia, 23–28 March 1980. [CrossRef]
24. Corredor, A.; Santos, M.; Peña, E.; Maciñeira, E.; Gómez-Martín, M.E.; Medina, J.R. Designing and Constructing Cubipod Armored Breakwaters in the Ports of Malaga and Punta Langosteira (Spain). In *From Sea to Shore-Meeting the Challenges of the Sea*; ICE Publishing: London, UK, 2014; pp. 518–527. [CrossRef]
25. Frostick, L.E.; McLelland, S.J.; Mercer, T.G. *Users Guide to Physical Modelling and Experimentation: Experience of The HYDRALAB Network*; CRC Press: Dundee, UK, 2011.
26. Phillips, O.M. On the dynamics of unsteady gravity waves of finite amplitude-Part The elementary interactions. *J. Fluid Mech.* **1960**, *9*, 193–217. [CrossRef]
27. Inman, D.; Munk, W.; Balay, M. Spectra of low frequency ocean waves along the Argentine shelf. *Deep Sea Res.* **1953**, *8*, 155–164. [CrossRef]
28. Mazzaretto, O.M.; Menéndez, M.; Lobeto, H. A global evaluation of the JONSWAP spectra suitability on coastal areas. *Ocean Eng.* **2022**, *266*. [CrossRef]
29. Kirkegaard, J.; Wolters, G.; Sutherland, J.; Soulsby, R.; Frostick, L. *Users Guide to Physical Modelling and Experimentation*; Taylor & Francis Group: Dundee, UK, 2011.
30. Losada, M.A.; Desire, J.M.; Alejo, L.M. Stability of blocks as breakwater stability of blocks as breakwater. *J. Struct. Eng.* **1986**, *112*, 2392–2401. [CrossRef]
31. Vidal, C.; Losada, M.A.; Medina, R. Stability of mound breakwater's head and trunk. *J. Waterw. Port Coast. Ocean Eng.* **1991**, *117*, 570–587. [CrossRef]
32. Putz, R.R. Statistical distributions for ocean waves. *Trans. Am. Geophys. Union* **1952**, *33*, 685–692. [CrossRef]
33. Goda, Y. Statistical Variability of Sea State Parameters as a Function of Wave Spectrum. *Coast. Eng. Jpn.* **1988**, *31*, 39–52. [CrossRef]
34. Via-Estrem, L.; Bunn, N.; Abernethy, R. Wave Spectra Revisited–New guidelines based on observations. In Proceedings of the Coasts, Marine Structures and Breakwaters, 5–7 September 2017; pp. 1177–1188. Available online: https://www.icevirtuallibrary.com/doi/abs/10.1680/cmsb.63174.1177 (accessed on 5 December 2022). [CrossRef]
35. USAERDC. *US Army Engineer Research and Development Centre. Coastal Engineering Manual, Part VI: Design of Coastal Project Elements (EM 1110-2-1100)*; USACE Publications: Washington, DC, USA, 2002.
36. Van der Meer, J.W.; Pilarczyk, K.W. Stability of Rubble Mound Slopes Under Random Wave Attack. In Proceedings of the 19th International Conference on Coastal Engineering, Houston, TX, USA, 3–7 September 1984. [CrossRef]